Molecular Modeling Studies Suggest That Zinc Ions Inhibit HIV-1 Protease by Binding at Catalytic Aspartates

Darrin M. York,[1,2] Tom A. Darden,[1] Lee G. Pedersen,[1,2] and Marshall W. Anderson[1]

[1]Laboratory of Molecular Toxicology, National Institute of Environmental Health Sciences, Research Triangle Park, NC 27709 USA; [2]Department of Chemistry, University of North Carolina at Chapel Hill, NC 27599-3290 USA

Human immunodeficiency virus type 1 protease is inhibited *in vitro* by zinc ions at neutral pH. The binding site of these ions is not known; however, experimental data suggest that binding may occur in the active site. To examine the possibility of zinc binding in the active site, molecular dynamics simulations in the presence and absence of zinc have been carried out to 200 psec. The results are compared with the 2.8-Å crystallographic structure of a synthetic HIV-1 protease, and a zinc binding site at the catalytic aspartate residues (Asp-25, Asp-25') is proposed. Molecular dynamics simulations show that the zinc ion remains stably bound in this region, coordinating the carboxylate side chains of both aspartate residues. Interaction with zinc does not disrupt the dimeric structure of the protein or significantly alter the structure of the active site. These data are consistent with experimental studies of HIV-1 protease inhibition by zinc and give strong evidence that this is the binding site that leads to inactivation.
Key words: active site, HIV-1, human immunodeficiency virus, ions, molecular dynamics models, protease, zinc. *Environ Health Perspect* 101:246–250(1993)

Human immunodeficiency virus type 1 protease (HIV-1 PR) is a 99-amino acid, virally encoded protein responsible for proteolytic cleavage of viral *gag* and *gag-pol* fusion polyproteins into functional products (*1–3*). The activity of the protease is required for viral infectivity *in vitro* (*4*). Consequently, HIV-1 PR is an attractive therapeutic target for rational drug design (*5,6*), and the focus of a tremendous amount of research.

HIV-1 PR has been characterized as an aspartic acid protease based on sequence homology to related enzymes (*7*), catalytic pH studies (*8*), and inhibition by well-known aspartyl protease inhibitors (*9,10*). The active form of the enzyme behaves as a dimer (*11,12*). These findings have been confirmed by the elucidation of X-ray crystallographic structures of the enzyme both unbound (*13–15*) and bound to synthetic inhibitors (*16–20*).

One feature that distinguishes the HIV-1 protease from cellular aspartyl proteases is the pH dependence of its activity. The optimum pH range for activity of the HIV-1 protease (4.5–6.0) (*8*) is considerably higher than for cellular enzymes *in vitro* (typically 2.0–4.0) (*21*). A notable exception is human renin, which has a pH optimum in the range of 5.5–7.5 (*22*). The pH optima of these enzymes presumably reflect the catalytic mechanism generally accepted for aspartyl proteases which requires one of the catalytic aspartate residues to be protonated. Recently, Zhang et al. (*23*) reported that zinc ions are inhibitors of both renin and HIV-1 PR at neutral pH. Although the zinc binding site(s) that lead to inactivation have not been determined, evidence suggests that one site may occur at or near the catalytic aspartate residues. In this study, molecular dynamics methodology was used to explore the possibility of zinc binding in the active site of HIV-1 PR and predict the effects of this binding on the structure. Our results are consistent with the requirements of zinc binding reported by Zhang et al. (*23*) and give supporting evidence that this is the site that leads to inhibition of the protease.

Methods

We performed molecular mechanics and dynamics calculations using a modified version of AMBER3.0 (Revision A) (*24,25*). The all-atom force field (*26*) was used for all standard residues, and solvent was treated explicitly using the TIP3P model (*27*). Parameters for chloride ions and zinc ions were taken from Lybrand et al. (*28*) and Bartolotti et al. (*29*), respectively. Electrostatic and van der Waals interactions were treated using a "twin range" (9/18 Å) residue-based cutoff, updated every 20 steps. We performed simulations under constant temperature (300 K) and pressure (1 bar) conditions using a 1-fsec integration time step, carried out to 200 psec.

We obtained the starting positions of the heavy atoms for the unbound and Zn^{2+}-bound dimers from the crystallographic structure of the synthetic ($Aba^{67,95}$) HIV-1 protease at pH 7.0 (*14*). The net charge of the unbound dimer was assumed to be +4, consistent with the normal protonation states of the component amino acids at neutral pH. It is possible that the active site aspartates share a proton near neutral pH, as maximum protease activity occurs in the range 4.5–6.0 (*8*). However, inflections in the log V/K versus pH profile observed at pH 3.1 and 5.2 suggest one of the aspartates is protonated at pH 5.2. Since we were simulating the protease at neutral pH, we chose to treat both aspartates as being fully charged in the simulations. In the case of the zinc-bound protease, it is reasonable to assume that Zn^{2+} ion binding (pK_a 9.5) (*30*) would involve both aspartates in the unprotonated form.

There was no particular bias in placing a Zn^{2+} ion in the active site *a priori*. Instead, the goal was to find the position of a Zn^{2+} ion resulting in the most favorable ion–protein potential energy based on the crystallographic coordinates for the protein heavy atoms (with hydrogens energy minimized by AMBER). Using this position for initial placement of the Zn^{2+} ion, molecular dynamics may then be used to refine the binding interactions and determine the resulting structural changes in the protein. Initial placement of a Zn^{2+} ion was determined by a grid search procedure, whereby the AMBER nonbond interaction energy (no cutoff) of the ion was tested on a 0.5 Å grid over a 5.0 Å box around the crystallographic structure. We used the grid points corresponding to the 1000 lowest energies as starting points for minimization of a single Zn^{2+} ion to a root mean square gradient tolerance of 0.000001 kcal/mol. The position corresponding to the global potential energy minimum was chosen for the placement of the ion. Interestingly, this procedure

Address correspondence to D. M. York, NIEHS, PO Box 12233, Research Triangle Park, NC 27709 USA. This work was funded in part by the University of North Carolina Medical School MD/PhD program, the National Cancer Institute, and the North Carolina Supercomputing Center. We thank A. Wlodawer for providing us with several crystallographic structures and for useful comments. We acknowledge grants of supercomputer time from the National Cancer Institute and the North Carolina Supercomputing Center. D.M.Y. thanks the University of North Carolina Medical School for support through the MD/PhD program. L.G.P. thanks NIEHS for support for this project and acknowledges NIH grant HL27995. We also thank Howard Smith at NIEHS for essential computer graphics assistance and Nobuko Hamaguchi and Paul Charifson for helpful suggestions.

resulted in the placement of the Zn^{2+} ion in the active site cleft directly between the carboxylate side chains of the catalytic aspartate residues.

The net charge of the protease and protease/ion complexes were neutralized with negatively charged chloride ions using the same procedure as for the zinc ion. The solute was solvated in a 13 Å water bath (8013 water molecules) and equilibrated using the same procedures as for previous simulations (*31*). Unconstrained dynamics was then performed on each system at constant pressure and temperature to 200 psec.

Results

Figure 1 shows the time evolution of the root mean square deviation of a carbon atoms with respect to the crystallographic structure for the molecular dynamics structures of the unbound and Zn^{2+}-bound protease. Both systems are well equilibrated after 150 psec. The unbound protease equilibrates with a carbon root mean square deviation of about 1.5 Å, whereas the Zn^{2+}-bound structure equilibrates at a lower value of approximately 1.2 Å. Secondary structural analysis of the crystallographic structure and the simulation (150–200 psec) average structures was performed using the Kabsch and Sander program DSSP (*32*). Of the 63 secondary structural assignments made for the crystallographic monomer, 46 (73%) were conserved in each monomer of the unbound structure, and 54 (86%) were conserved in each monomer of the Zn^{2+}-bound structure.

Table 1. Hydrogen bonding at the dimer interface

Contact atom 1–atom 2	X-ray Distance (Å)	Zn^{2+} bound Distance (Å)	Zn^{2+} bound % Time bonded	Unbound Distance (Å)	Unbound % Time bonded
Pro-1 HN^{+}-Phe-99 O	1.71	1.79	100	1.73	100
		1.76	100	2.85	46
Pro-1 O-Phe-99 HN	2.16	2.13	86	2.07	93
		—	—	—	—
Ile-3 HN-Leu-97 O	1.68	2.12	88	2.09	88
		2.12	88	2.03	93
Ile-3 O-Leu-97 HN	1.78	1.97	97	1.97	99
		1.96	100	1.97	99
Leu-5 O-Arg-87 HN21	2.16	1.97	96	2.03	87
		1.91	98	3.39	28
Trp-6 O-Arg-87 HN22	—	2.23	66	2.60	16
		2.09	88	3.81	13
Leu-24 O-Thr-26 HOG	2.55	1.90	99	2.05	93
		1.88	100	1.91	100
Thr-26 HN-Thr-26 OG1	2.22	2.02	98	2.29	65
		2.05	98	2.03	93
Gly-49 HN-Gly-51 O	—	—	—	2.06	94
		—	—	—	—
Gly-51 HN-Gly-51 O	2.42	—	—	1.99	100
		—	—	—	—
His-69 HNE-Phe-99 OXT	2.49	—	—	—	—
		1.99	89	—	—
Thr-96 HN-Asn-98 O	2.41	2.03	93	2.00	98
		2.03	95	2.01	99
Thr-96 O-Asn-98 HN	2.02	2.00	98	1.94	99
		2.03	93	1.96	99

Hydrogen bonds at the dimer interface in the HIV-1 PR crystallographic structure and in the simulations. Hydrogens were added to the crystallographic structure (X-ray) using AMBER and energy minimized keeping the nonhydrogen positions fixed. In the unbound and Zn^{2+}-bound simulations, the average H-bond distances and percent time the H bond was maintained [definition of an H bond as in York et al. (*31*)] are listed for each monomer (monomer 1 is listed on the same line as the H-bond atoms, monomer 2 is listed immediately below).

Hydrogen Bonding at the Dimer Interface

An analysis of H-bond contacts at the dimer interface over the last 50 psec of the simulations has been performed (Table 1). The primary hydrogen bond interactions at the dimer interface (*33*) present in the crystallographic structure are maintained in solution both in the unbound and Zn^{2+}-bound simulations. These include interactions at the amino- and carboxy-terminal ß strands (residues 1–4, 95–99), which form a four-stranded antiparallel B sheet, and in the region of the active site triads (residues 25–27), which interlock in the "fireman's grip" characteristic of aspartyl proteases (*33*). In particular, inter-subunit hydrogen bonds involving residues at or near the active site (Leu-24, Thr-26, and Arg-87) were all maintained in the presence of bound zinc.

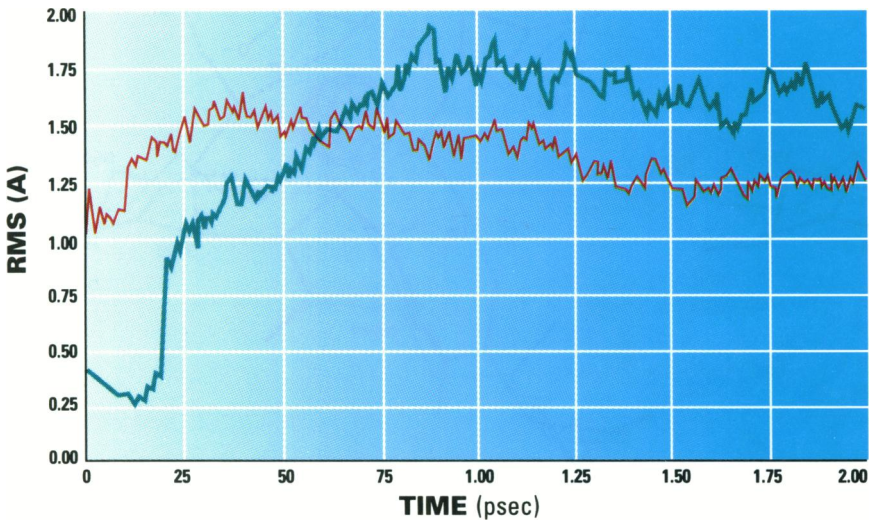

Figure 1. Time evolution of the α carbon root mean square deviation from the crystallographic structure of Wlodawer et al. (*14*) for the unbound protease simulation (thick line) and the Zn^{2+}-bound protease simulation (thin line).

Zinc–Protein Interaction

Figure 2 shows the pair distribution function (*34*), $g_{ab}(r)$, for the carboxylate oxygens of the catalytic aspartate residues (Fig. 2a) and water oxygens (Fig. 2b) around the Zn^{2+} ion and the corresponding running integration numbers, which indicate the average number of oxygens of each type in a sphere of radius r around the ion. The pair distribution function for the carboxylate oxygens shows a single, sharp peak centered at 2.13 Å, and the corresponding coordination number, indicated by the running integration number, is 4. The pair distribution function for water oxygens shows there are three water molecules associated with the zinc ion in its first sol-

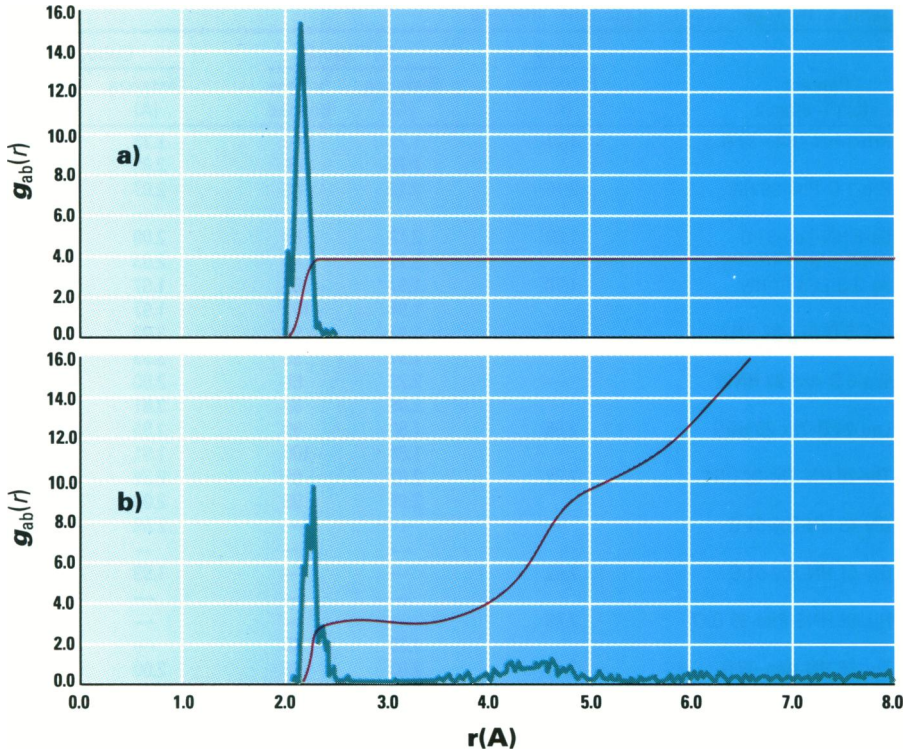

Figure 2. Pair distribution function (*34*), $g_{ab}(r)$, of oxygens around the zinc ion during the final 50 psec of the Zn^{2+}-bound simulation (thick lines) for (a) carboxylate oxygens of the catalytic aspartates and (b) water oxygens. The corresponding running integration numbers are also shown (thin lines).

vation sphere at a distance of around 2.25 Å. No exchange of oxygens in the first coordination sphere of zinc was observed during the last 50 psec of the simulation. Zinc has been observed to be coordinated to multiple carboxylate ligands in other enzymes such as DNA polymerase I from *Escherichia coli* (*35*).

Figure 3 is a stereo picture of the active-site triads at the dimer interface with the Zn^{2+} ion bound to the catalytic aspartates. The crystallographic structure of Wlodawer et al. (*14*) is also shown superimposed. Inter-subunit H bonds between Thr-26→Leu-24′ and between Thr-26 ←Thr-26′ (primes indicate residues of the symmetry-related monomer), termed the "fireman's grip," are clearly maintained. Additionally, the OD1 atoms of the aspartate side chains maintain H-bond contact with the backbone amino group of Gly-27 on the same strand. These H bonds are also pronounced in the crystallographic structure.

The flap regions of the protease (residues 42–58), which are observed in crystallographic structures to significantly rearrange upon inhibitor binding (*16–20*), were not observed to interact with the zinc ion in the simulation. Examination of the

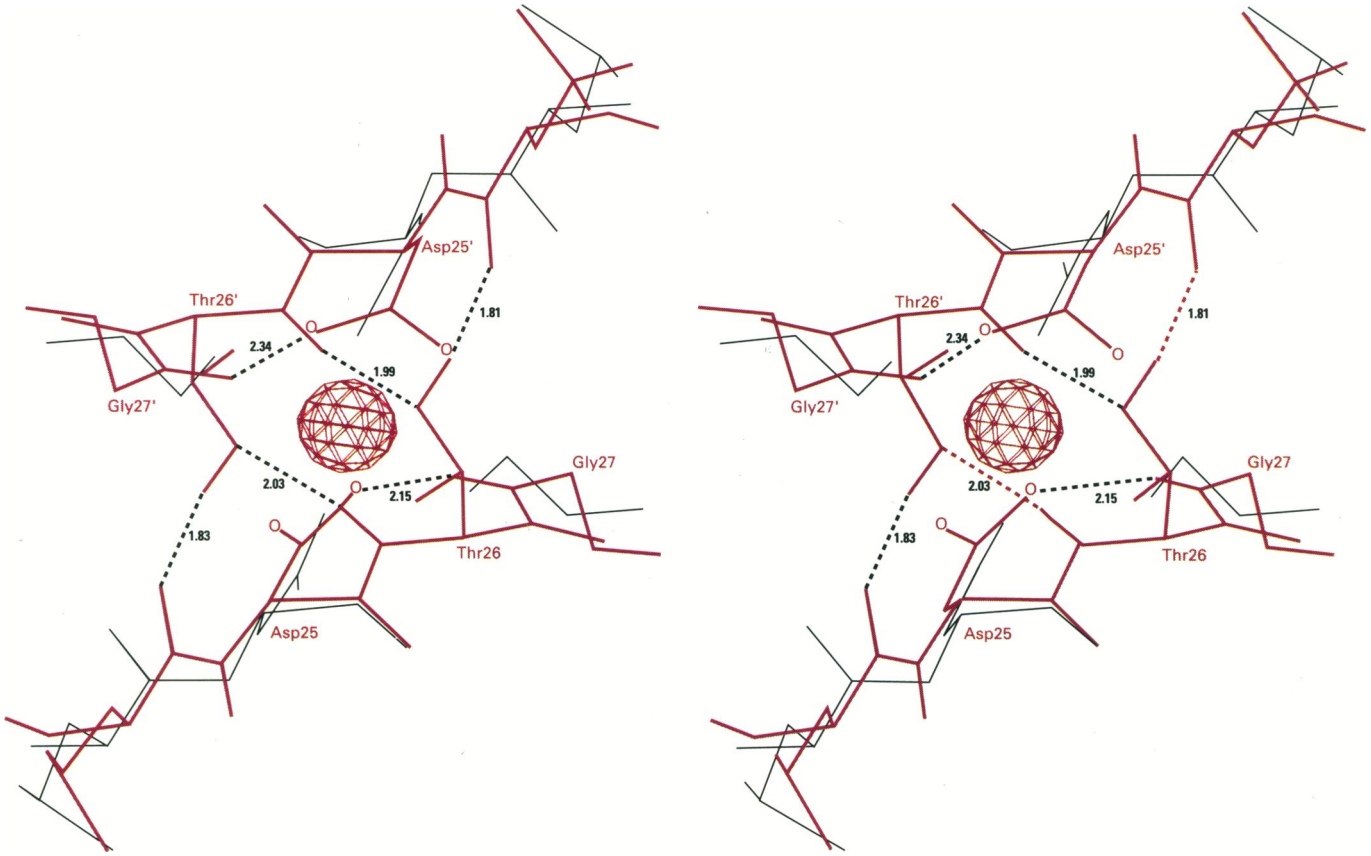

Figure 3. Stereo picture of the active site triads (residues 25–27 and the corresponding symmetry related residues) for the 150–200 psec Zn^{2+}-bound average structure showing zinc ion binding to the active site aspartates. The carboxylate oxygens of the catalytic aspartates are labeled "O," and inter-subunit hydrogen bonds are indicated by dotted lines [$r_{Zn^{2+}\text{-}O}$ = 2.13, 2.14 Å (Asp-25); 2.10, 2.14 Å (Asp-25′)].

average structure of the zinc-bound protease indicates the nearest backbone atoms of the flaps reside more than 9 Å away from the zinc ion.

Discussion

Kinetic studies have shown that zinc is an effective inhibitor of renin and HIV-1 PR at pH 7, two aspartyl proteases with pH optima near neutrality (*23*). Other studies of metal ion inhibition of HIV-1 PR performed at pH 5 did not reveal significant inhibition of the enzyme by Zn^{2+} ions (*36*). If inhibition of HIV-1 PR is a result of Zn^{2+} binding at the active-site aspartate residues, it is reasonable to expect that conditions that favor both aspartates in the unprotonated form would enhance Zn^{2+} binding, and hence inhibition. Because both catalytic aspartates presumably are unprotonated around neutrality, the observed pH dependence of Zn^{+2} inhibition is consistent with binding at or near the catalytic aspartates. Although the bacterially expressed HIV-1 PR has three residues that commonly bind zinc (Cys-67, His-69, and Cys-95), Zn^{2+} also inhibits the related HIV-2 protease, which does not contain cysteines or histidines [for a discussion of HIV-2 protease, see Gustchina and Weber (*37*) and Tomasselli et al. (*38*)], in an identical manner as the HIV-1 protease (*23*). This suggests that these residues are not required binding sites for inactivation by zinc. Considered with the fact that inhibition was observed to be first order (*23*) in Zn^{2+}, we may infer that there is a single important binding site that causes inactivation. Furthermore, inactivation of the protease by zinc was observed to be reversible, as protease activity could be restored upon addition of EDTA (*23*), which has a higher affinity than carboxylate moieties for Zn^{2+} ions. These data are, therefore, consistent with the requirement of noncovalent binding of Zn^{2+} in the active site.

The present study of Zn^{2+} binding at the catalytic aspartate residues provides evidence that this is the site responsible for inactivation of the protease. Evaluation of the potential energy of a Zn^{2+} ion in the field of the crystallographic structure suggests a probable binding site for zinc occurs in the active site at the catalytic aspartates (see Methods). Subsequent molecular dynamics simulations predict that the zinc ion remains stably bound in this region; i.e., no exchange of carboxylate oxygens was observed in the first coordination sphere of the zinc ion after initial equilibration. Because the hydrolysis mechanism mediated by HIV-1 PR requires one of the aspartates to be protonated, forming a hydrogen bond with the carbonyl oxygen of the scissile bond and the other in the unprotonated form to activate a water molecule for hydrolysis (*6*), the coordination of both of these residues by a zinc ion would conceivably inactivate the enzyme. Gel filtration and equilibrium sedimentation analyses suggest that zinc binding does not involve disruption of the dimeric structure of the protease (*23*). Our simulation with bound Zn^{2+} shows no weakening of the dimer. The overall simulation results indicate that Zn^{2+} can bind stably with the catalytic aspartate residues of the HIV-1 protease without significantly disrupting the overall structure. These results are consistent with experimental studies and taken together suggest that the site of Zn^{2+} binding that leads to catalytic inhibition is the active site.

References

1. Henderson LE, Copeland TD, Sowder RC, Schultz AM, Oroszlan S. Analysis of proteins and peptides from sucrose gradient banded HTLV-III. In: Human retroviruses, cancer, and AIDS: approaches to prevention and therapy (Bolognesi D, ed). New York: Alan R. Liss, 1988;135–147.
2. Debouck C, Gorniak JG, Strickler JE, Meek TD, Metcalf BW, Rosenberg M. Human immunodeficiency virus protease expressed in *Escherichia coli* exhibits autoprocessing and specific maturation of the *gag* precursor. Proc Natl Acad Sci USA 84:8903–8906(1987).
3. Graves MC, Meidel MC, Pan YC, Manneberg M, Lahm HW, Gruninger-Leitch F. Identification of a human immunodeficiency virus-1 protease cleavage site within the 66,000 dalton subunit of reverse transcriptase. Biochem Biophys Res Commun 168:30–36 (1990).
4. Kohl NE, Emini EA, Scheif WA, Davis LJ, Heimbach JC, Dixon RA, Scolnick EM, Sigal IS. Active human immunodeficiency virus protease is required for viral infectivity. Proc Natl Acad Sci USA 85:4686–4690(1988).
5. Huff J. HIV protease: a novel chemotherapeutic target for AIDS. J Med Chem 34: 2305– 2314(1991).
6. Debouck C. The HIV-1 protease as a therapeutic target for AIDS. (1992) AIDS Hum Retroviruses 8:153–164(1992).
7. Toh H, Kikuno R, Hayashida H, Miyata T, Kugimiya W, Inouye S, Yuki S, Saigo K. Close structural resemblance between putative polymerase of a drosophila transposable genetic element 17.6 and pol gene product of Moloney murine leukaemia virus. EMBO J 4:1267– 1272(1985).
8. Hyland LJ, Tomaszek TA, Meek TD. Human immunodeficiency virus-1 protease. 2. Use of pH rate studies and solvent kinetic isotope effects to elucidate details of chemical mechanism. Biochemistry 30:8454–8463(1991).
9. Seelmeir S, Schmidt H, Turk V, von der Helm K. Human immunodeficiency virus has an aspartic-type protease that can be inhibited by pepstatin A. Proc Natl Acad Sci USA 85:6612– 6616(1988).
10. Richards AD, Roberts R, Dunn BM, Graves MC, Kay J. Effective blocking of HIV-1 protease activity by characteristic inhibitors of aspartic proteinases. FEBS Lett 247:113–117(1989).
11. Darke PL, Leu CT, Davis LJ, Heimbach JC, Diehl RE, Hill WS, Dixon RA, Sigal IS. Human immunodeficiency virus protease. Bacterial expression and characterization of the purified aspartic protease. J Biol Chem 264: 2307–2312(1989).
12. Meek TD, Dayton BD, Metcalf BW, Dreyer GB, Strickler JE, Gorniak JG, Rosenberg M, Moore M, Magaard VW, Debouck C. Human immunodeficiency virus 1 protease expressed in *Escherichia coli* behaves as a dimeric aspartic protease. Proc Natl Acad Sci USA 86:1841–1845(1989).
13. Navia MA, Fitzgerald PMD, McKeever BM, Leu C-T, Heimbach JC, Herber WK, Sigal IS, Darke PL, Springer JP. Three-dimensional structure of aspartyl protease from human immunodeficiency virus HIV-1. Nature 37: 615–620(1989).
14. Wlodawer A, Miller M, Jaskólski M, Sathyanarayana BK, Baldwin E, Weber IT, Selk LM, Clawson L, Schneider J, Kent SBH. Conserved folding in retroviral proteases: crystal structure of a synthetic HIV-1 protease. Science 245:616–621(1989).
15. Lapatto R, Blundell T, Hemmings A, Overington J, Wilderspin A, Wood S, Merson JR, Whittle PJ, Danley DE, Geoghegan KF, Hawrylik SJ, Lee SE, Scheld KG, Hobart PM. X-ray analysis of HIV-1 proteinase at 2.7 Å resolution confirms structural homology among retroviral enzymes. Nature 342:299–302 (1989).
16. Miller M, Schneider J, Sathyanarayana BK, Toth MV, Marshal GR, Clawson L, Selk L, Kent SB, Wlodawer A. Structure of complex of synthetic HIV-1 protease with a substrate-based inhibitor at 2.3 Å resolution. Science 246:1149–1152(1989).
17. Fitzgerald PM, McKeever BM, VanMiddlesworth JF, Springer JP, Heimbach JC, Leu CT, Herber WK, Dixon RA, Darke PL. Crystallographic analysis of a complex between human immunodeficiency virus type 1 protease and acetyl-pepstatin at 2.0 Å resolution. J Biol Chem 265:14209–14219(1990).
18. Swain AL, Miller MM, Green J, Rich DH, Schneider J, Kent SB, Wlodawer A. X-ray crystallographic structure of a complex between a synthetic protease of human immunodeficiency virus 1 and a substrate-based hydroxyethylamine inhibitor. Proc Natl Acad Sci USA 87:8805–8809(1990).
19. Erickson J, Neidhart DJ, VanDrie J, Kempf DJ, Wang XC, Norbeck DW, Plattner JJ, Rittenhouse JW, Turon M, Wildeburg N, Kohlbrenner WE, Simmer R, Helfrich R, Paul DA, Knigge M. Design, activity, and 2.8 Å resolution crystal structure of a C_2 symmetric inhibitor complexed to HIV-1 protease. Science 249:527–533(1990).
20. Jaskólski M, Tomasselli AG, Sawyer TK, Staples DG, Heinrikson RL, Schneider J, Kent SB, Wlodawer A. Structure at 2.5-Å resolution of a chemically synthesized human immunodeficiency virus type 1 protease complexed with a hydroxyethylene-based inhibitor. Biochemistry 30:1600–1609(1991).
21. Ido E, Han H, Kezdy FJ, Tang J. Kinetic studies of human immunodeficiency virus type 1 protease and its active-site hydrogen bond mutant A28S. J Biol Chem 266:24359–24366 (1991).
22. Inagami T. Renin. In: Biochemical regulation of blood pressure (Soffer RL, ed). New York: John Wiley and Sons, 1981;39–73.
23. Zhang Z, Reardon I, Hui J, O'Connell K, Poorman R, Tomasselli A, Heinrikson R. Zinc

inhibition of renin and the protease from human immunodeficiency virus type 1. Biochemistry 36:8717–8721(1991).
24. Weiner SJ, Kollman PA, Case DA, Singh UC, Chio C, Alagona G, Profeta S, Weiner P. A new force field for molecular mechanical simulation of nucleic acids and proteins. J Am Chem Soc 106:765–784(1984).
25. Foley CK, Pedersen LG, Charifson PS, Darden TA, Wittinghofer A, Pai EF, Anderson MW. Simulation of the solution structure of the H-ras p21-GTP complex. Biochemistry 31:4951–4959(1992).
26. Weiner SJ, Kollman PA. An all atom force field for simulations of proteins and nucleic acids. J Comput Chem 7:230–252(1986).
27. Jorgensen WL, Chandrasekhar J, Madura JD, Impey RW, Klein ML. Comparison of simple potential functions for simulating liquid water. J Chem Phys 79:926–935(1983).
28. Lybrand T, McCammon J, Wipff G. Theoretical calculation of relative binding affinity in host-guest systems. Proc Natl Acad Sci USA 83:833–835(1986).
29. Bartolotti L, Pedersen L, Charifson P. Long range nonbonded attractive constants for some charged atoms. J Comput Chem 12:1125–1128(1991).
30. Burgess, J. Ions in solution. New York: John Wiley and Sons, 1988.
31. York D, Darden T, Pedersen L, Anderson M. Molecular dynamics simulation of HIV-1 protease in a crystalline environment and in solution. Biochemistry 32:1443–1453(1993).
32. Kabsch W, Sander C. Dictionary of protein secondary structure: pattern recognition of hydrogen-bonded and geometrical features. Biopolymers 22:2577–2637(1983).
33. Weber IT. Comparison of the crystal structure and intersubunit interactions of human immunodeficiency and Rous sarcoma virus proteases. J Biol Chem 265:10492–10496 (1990).
34. Allen MP, Tildesley DJ. Computer simulations of liquids. New York:Oxford University Press, 1987.
35. Beese LS, Steitz TA. Structural basis for the 3'-5' exonuclease activity of *Escherichia coli* DNA polymerase I: a two metal ion mechanism. EMBO J 10:25–33(1991).
36. Woon T, Brinkworth R, Farlie D. Inhibition of HIV-1 proteinase by metal ions. Int J Biochem 24:911–914(1992).
37. Gustchina A, Weber IT. Comparative analysis of the sequences and structures of HIV-1 and HIV-2 proteinases. Proteins 10:325–339 (1991).
38. Tomasselli AG, Hui JO, Sawyer TK, Staples DJ, Bannow C, Reardon IM, Howe WJ, DeCamp DL, Craik CS, Heinrikson RL. Specificity and inhibition of proteases from human immunodeficiency viruses 1 and 2. J Biol Chem 265:14675–14683(1990).